Original Article

Asian Pacific Journal of Tropical Biomedicine

apjtb.org

doi: 10.4103/2221-1691.378601

Impact Factor® 1.51

G9a-targeted chaetocin induces pyroptosis of gastric cancer cells

Mian-Qing Huang[1,2]✉, Gui-Lan Tao[3], Li-Fang Han[2], Shu-Hong Tian[2], Peng Zhou[4]✉

[1]*School of Life Science, Hainan University, Haikou, China*

[2]*Center for Drug Safety Evaluation, Hainan Medical University, Haikou, China*

[3]*The First Affiliated Hospital of Hainan Medical University, Haikou, China*

[4]*Key Laboratory of Biology and Genetic Resources of Tropical Crops, Ministry of Agriculture and Rural Affairs & Institute of Tropical Bioscience and Biotechnology, Chinese Academy of Tropical Agricultural Sciences, Haikou, China*

ABSTRACT

Objective: To evaluate the effect of chaetocin on pyroptosis of gastric cancer cells and its underlying mechanisms.

Methods: The proliferation of gastric cancer cells was detected by trypan blue staining. Flow cytometry and Hoechst/propidium iodide double staining were used to detect apoptosis and pyroptosis. Cellular ultrastructure was observed by transmission electron microscopy. The levels of p-mixed lineage kinase domain-like (MLKL), gasdermin-D (GSDMD), gasdermin E (GSDME), *N*-GSDMD, and *N*-GSDME proteins were detected by Western blotting. In addition, lactate dehydrogenase (LDH) release assay was used to verify pyroptosis induced by chaetocin, and caspase 3 inhibition test and siRNA interference test were conducted to investigate pyroptosis mechanisms.

Results: Chaetocin at concentrations of 200 nmol/L to 600 nmol/L inhibited the proliferation of AGS, HGC27, MKN28, and SGC7901 gastric cancer cells in a dose-dependent and time-dependent manner by inducing apoptosis and pyroptosis. Significant ultrastructure changes, such as chromatin condensation, vacuolization, disrupted mitochondrial cristae, and increased nuclear occupancy, were observed after treatment with chaetocin in SGC7901 cells. Chaetocin at a concentration of 400 nmol/L significantly increased the number of pyroptotic cells, LDH release, and the ratio of *N*-GSDME/GSDME ($P<0.01$), which were reversed by Z-DEVD-FMK. In addition, chaetocin did not affect the expression of GSDMD. G9a silencing abolished the effect of chaetocin on the expression levels of GSDME and *N*-GSDME and LDH release ($P>0.05$).

Conclusions: In addition to inducing apoptosis, chaetocin inhibits gastric cancer cells by inducing pyroptosis *via* the caspase 3/GSDME pathway. G9a was the target of chaetocin to induce pyroptosis of gastric cancer cells.

KEYWORDS: Chaetocin; Gastric cancer; Pyroptosis; G9a; GSDME

1. Introduction

Gastric cancer is a major threat to human health with a 5-year survival rate of less than 20%. Global cancer statistics released by the International Agency for Research on Cancer under the GLOBOCAN 2020 program reported gastric cancer as the fifth most common with 1 089 103 new cases and a morbidity rate of 5.6%.

Significance

Chaetocin induces apoptosis of many types of tumor cells. The current study demonstrated that chaetocin induced pyroptosis of gastric cancer cells *via* the caspase 3/GSDME pathway and G9a was the target of chaetocin to induce pyroptosis. Therefore, chaetocin can be further explored in combination with other chemotherapy drugs and developed as an anti-tumor agent.

✉To whom correspondence may be addressed. E-mail: 792015216@qq.com (MQ. Huang); zhp6301@126.com (P. Zhou)

How to cite this article: Huang MQ, Tao GL, Han LF, Tian SH, Zhou P. G9a-targeted chaetocin induces pyroptosis of gastric cancer cells. Asian Pac J Trop Biomed 2023; 13(6): 268-276.

Article history: Received 7 April 2023; Revision 28 April 2023; Accepted 15 June 2023; Available online 26 June 2023

The mortality was 7.7% in 2020, accounting for 768 793 deaths and making this the fourth most deadly cancer[1]. Early diagnosis of gastric cancer is difficult and most patients are diagnosed at an advanced stage. Furthermore, the efficacy of anti-gastric cancer drugs is unsatisfactory and surgical treatment is the last resort for most patients[2]. Therefore, there is an urgent need to develop superior anti-gastric cancer medicines.

G9a, a histone methyl transferase (HMT) generates H3K9me1 and H3K9me2 by transferring a methyl group from S-adenosylmethionine to histone H3 at lysine K9 (H3K9). The resulting modification has gene regulatory effects[3,4]. G9a is encoded by the *EHMT2* gene and belongs to the Su (var)3-9, Enhancer-of-zeste, Trithorax (SET) domain-containing Su(var)3-9 family. Its *N*-terminus contains Pre-SET, I-SET, and Post-SET domains with characteristic ankyrin repeats[5,6]. In order to explore the relationship between G9a expression and the prognosis of patients, a search was performed on the Kaplan Meier Plotter website. High G9a expression in tumor tissues was associated with a significantly reduced survival rate and mean survival time, suggesting an impact of G9a on gastric cancer progression.

Chaetocin is biosynthesized by the fungus, *Chaetomium*, and is a naturally-occurring HMT inhibitor[7,8]. Dithiodiketopiperazine rings contribute to its pharmacological effects, such as anti-tumor activity and reversal of HIV latency[9]. Chaetocin is thought to induce apoptosis, contributing to its anti-tumor cytotoxicity, but no reports on tumor cell pyroptosis have been found[10–12]. Therefore, the current study aimed at investigating the effect of chaetocin on pyroptosis of gastric cancer cells and its underlying mechanisms.

2. Materials and methods

2.1. Reagents and antibodies

The reagents and antibodies were used as follows: Chaetocin and Z-DEVD-FMK (Selleck Chemicals, Shanghai, China), anti-mixed lineage kinase domain-like (MLKL) (phospho S358), anti-cleaved *N*-terminal gasdermin-D (GSDMD), anti-cleaved *N*-terminal gasdermin E (GSDME), anti-G9a (Abcam, Cambridge, UK), anti-beta-actin primary antibodies and HRP-conjugated secondary antibody (Servicebio Technology, Wuhan, China).

2.2. Cell culture

Gastric cancer cell lines AGS (poorly differentiated), HGC27 (undifferentiated), MKN28, (highly differentiated) and SGC7901 (moderately differentiated) were purchased from Otwo Biotech (Otwo Biotech, Shenzhen, China) and cultured in RPMI 1640 medium (Hyclone, Utah, USA) with 10% fetal bovine serum (Tianhang, Huzhou, China) at 37℃ in a humidified environment with 5% CO_2.

2.3. Cell viability

Aliquots of 1×10^5 cells were seeded into 24-well plates and cultured for 24 h. Cells from 3 wells were harvested at 24 h, 48 h, 72 h, 96 h, and 120 h for viability measurement by staining with 0.08% trypan blue (Solarbio, Beijing, China) for 2 min at room temperature and counting in a hemocytometer under an inverted microscope.

2.4. Flow cytometry

Cells were digested, centrifuged, and washed with phosphate-buffered saline (PBS). Cell death was detected by flow cytometry based on Annexin V-FITC/propidium iodide (PI) double labeling following the instructions of the FITC Annexin-V Apoptosis Detection Kit (BD Biosciences, San Diego, CA, USA)[13]. Caspase 3 activity was suppressed in gastric cancer cells with Z-DEVD-FMK (ZDF) to distinguish GSDMD or GSDME pyroptotic pathway. Cells were treated with chaetocin at different concentrations for 24 h immediately after incubating with 50 μmol/L ZDF for 30 min. Stained cells were detected by BD Accuri C6 flow cytometer (BD Biosciences) and results were analyzed by BD Accuri C6 software.

2.5. Hoechst/PI double staining

Cells were cultured in 24-well plates. Then the medium was removed and washed with PBS before double-staining with Hoechst 33342/PI for 20 min according to the instructions of the Hoechst 33342/PI Double Staining Kit (Solarbio, Beijing, China). Fluorescence was assessed by ZEISS Axio Vert.A1 fluorescence microscope.

2.6. Transmission electron telescope

SGC7901 cells were treated with chaetocin for 24 h and gently scraped into suspension in clean 1.5 mL EP tubes and centrifuged at 1 500 rpm for 10 min. The supernatant was discarded and the cells were fixed with 2.5% fresh glutaraldehyde. Ultrathin sections were made for staining, as described previously[14], and photographed with a Hitachi JEM-1400 Flash transmission electron microscope.

2.7. Western blotting

Cells were harvested, centrifuged, and washed with PBS, and cell lysates containing phenylmethylsulfonyl fluoride and

phosphoprotease inhibitors were prepared. Protein concentrations were determined in a loading buffer with BCA protein quantitative assay kit (Servicebio). The proteins were separated by electrophoresis on 10% polyacrylamide gel (Servicebio) and electroporated onto PVDF membranes (Servicebio), blocked with 5% skimmed dry milk for 2 h, and incubated with primary antibodies against p-MLKL (ab187091; 1∶1 000; Abcam), *N*-GSDMD (ab215203; 1∶1 000; Abcam), *N*-GSDME (ab196436; 1∶1 000; Abcam), G9a (ab185050; 1∶1 000; Abcam) and β-actin (GB15001; 1∶1 500; Servicebio) overnight and secondary antibody conjugated with horseradish peroxidase (GB23301; 1∶4 000; Servicebio) for 2 h. Protein bands were visualized for luminescence with an ECL Kit (Servicebio), scanned, and analyzed with a Tanon-5200Multi gel imaging system (Tanon, Shanghai, China). The optical density values of the target bands were analyzed using ImageJ software (National Institutes of Health)[15].

2.8. Lactate dehydrogenase (LDH) release

After cells were treated with chaetocin for 24 h, LDH activity in the medium was measured according to the instructions of the LDH Cytotoxicity Assay Kit (Yeasen, Shanghai, China). The percentage of LDH activity was calculated as the ratio of LDH OD_{490} in the cell medium to total cellular LDH with optical densities determined by a microplate reader (Thermo Fisher Scientific).

2.9. siRNA knockdown

Two siRNAs (Invitrogen) for silencing of the *EHMT2* gene encoding G9a were synthesized with the sequences: siEHMT2-1: 5′-GCACAAGCACATCGAGGTGAT-3′, siEHMT2-2: 5′-GCAACATCAGCCGCTTCATCA-3′. Aliquots of 1×10^5 SGC7901 cells were seeded into 6-well plates and grown for 24 h before transfection with 50 pmol siRNA for 72 h, as directed by the instructions of Lipofectamine RNAiMAX (Invitrogen). Cells were treated with 400 nmol/L chaetocin and Western blotting and LDH release assays were performed 24 h later.

2.10. Bioinformatics analysis

The GEPIA website (http://gepia.cancer-pku.cn) was used to analyze the differential expression of *EHMT2* gene between normal gastric tissue and gastric cancer.

2.11. Statistical analysis

Statistical analyses were performed using GraphPad Prism version 7.0 for Windows and data are expressed as mean ± standard deviation (SD). One-way ANOVA was used to assess statistical differences between the two groups. A value of $P<0.05$ was considered statistically significant.

3. Results

3.1. Chaetocin inhibits the proliferation of gastric cancer cells

Treatment with 50, 100, 200, 400, and 600 nmol/L chaetocin produced a time-dependent decline in survival rates of AGS and SGC7901 cells (Figure 1A and D). The survival rate of AGS and SGC7901 cells was zero after 120 h of treatment with 400 nmol/L chaetocin. The viability of SGC7901 cells was declined with increasing concentration. Cell morphology changed from normal to aberrant, such as rounding, vacuolization, detached cells (Figure 1E). AGS cells showed the greatest sensitivity to all doses of chaetocin cytotoxicity with fewer than 40% survival rate after 24 h of treatment (Figure 1A). Surprisingly, the viability of HGC27 and MKN28 cells was increased after treatment with 50 nmol/L chaetocin for 24-72 h. Whereas at 100-600 nmol/L, chaetocin inhibited the viability of HGC27 and MKN28 cells in a time- and concentration-dependent manner (Figure 1B and C).

3.2. Chaetocin induces apoptosis and pyroptosis of gastric cancer cells

The quadrant of Annexin V-FITC single staining (blue) indicated apoptotic cells and double-stained (green) cells had incomplete cell membranes due to the occurrence of necrosis or pyroptosis. Figure 2A shows that chaetocin induced apoptosis in four gastric cancer cells, with the most significant proapoptotic effects on AGS cells at 200 nmol/L and SGC7901 cells at 400 nmol/L. Chaetocin also induced other cell death with incomplete cell membranes, with the best effect in all four cell lines at a concentration of 400 nmol/L. The data of flow cytometry demonstrated that SGC7901 cells had the lowest spontaneous mortality rate among the four cell lines, thus the following mechanism study was conducted mainly on this cell line. The level of p-MLKL, a necrosis marker protein was not altered in AGS, HGC27, MKN28, and SGC7901 cells following 24 h of 400 nmol/L chaetocin treatment (Figure 2C). Thus, cells showing Annexin V-FITC/PI double staining can only be pyroptotic. This result was further confirmed by the subsequent detection of the pro-pyroptotic protein, GSDME. The combination of p-MLKL and flow cytometry results indicated that chaetocin induced both apoptosis and pyroptosis simultaneously in gastric cancer cells. The merged pink fluorescence images by Hoechst 33342/PI double staining also identified SGC7901 cells with incomplete cell membranes (Figure 2B) which were also pyroptotic and the

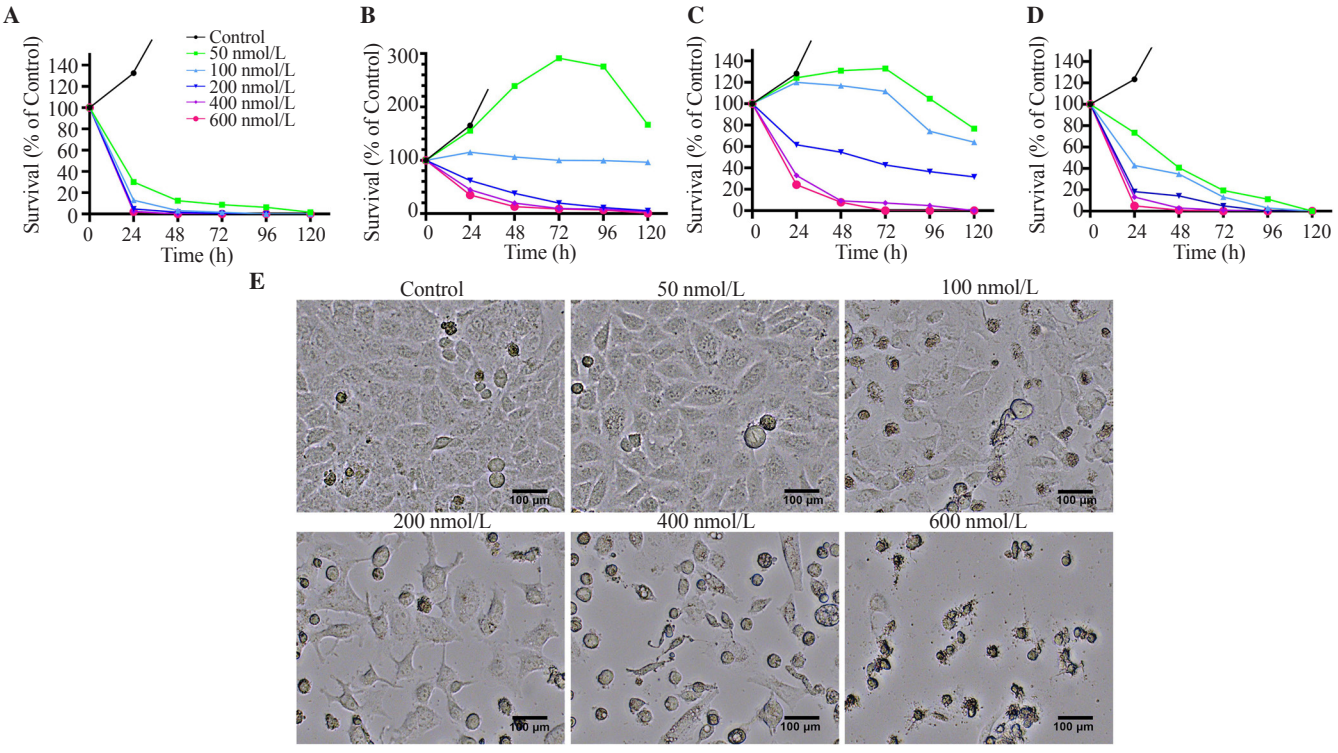

Figure 1. Chaetocin inhibits the proliferation of gastric cancer cells (A: AGS, B: HGC27, C: MKN28, and D: SGC7901). Four gastric cancer cell lines were treated with chaetocin at 50-600 nmol/L and observed for 24-120 h by trypan blue staining under a microscope. Cell survival ratios at different times were calculated to plot the dose-response-time curves. (E) Cellular morphology was observed after chaetocin treatment at different concentrations for 24 h and the representative images of SGC7901 cells are shown at a magnification of 200×.

number of pyroptotic SGC7901 cells was increased with increasing chaetocin concentration. Ultrastructural examination of SGC7901 cells by transmission electron microscope revealed that chaetocin induced noticeable changes in SGC7901 cells. Control untreated SGC7901 cells had well-ordered organelles with typical structures and a relatively small nuclear volume. Treatment with 100 nmol/L chaetocin increased the nucleus-to-cytoplasm ratio accompanied by apoptotic characteristics, such as chromatin condensation, intermediate vacuolization, and a decreased number of abnormally shaped mitochondria. SGC7901 cells exposed to 200 nmol/L chaetocin had more increased chromatin condensation, massive cytoplasm vacuolization, few organelles, disrupted mitochondrial cristae, and increased nuclear occupancy. Large-scale nuclear membrane disruption, intranuclear vacuolization, visible chromatin in the cytoplasm, severe cytoplasmic vacuolization, and almost no organelles with intact structures could be seen after treatment with 400 nmol/L chaetocin (Figure 2D). Although the cell volume did not alter greatly compared with untreated SGC7901 cells, the chaetocin-treated cells had noticeably increased nuclear occupancy. In summary, chaetocin promoted pyroptosis of gastric cancer cells in addition to inducing apoptosis.

3.3. The caspase 3/GSDME signaling pathway is involved in chaetocin–induced pyroptosis in gastric cancer cells

Caspase 3 activity was suppressed in AGS, HGC27, MKN28, and SGC7901 cells with ZDF to distinguish between GSDMD and GSDME pyroptotic pathways. Treatment with 400 nmol/L chaetocin increased the number of pyroptotic cells (P<0.01), which was reversed by ZDF in all gastric cancer cell lines except HGC27 (P<0.01) (Figure 3A). LDH release was evaluated to confirm pyroptosis. Chaetocin treatment caused an increase in LDH release (P<0.01), however, ZDF substantially inhibited this effect (P<0.01) (Figure 3B). Thus, the results suggest the involvement of caspase 3 in chaetocin-induced pyroptosis. GSDME, *N*-GSDME, GSDMD, and *N*-GSDMD levels in SGC7901 cells were assessed by Western blotting. Chaetocin treatment raised GSDME and *N*-GSDME levels but did not affect GSDMD and *N*-GSDMD levels. ZDF inhibited the upregulation of GSDME and *N*-GSDME levels caused by chaetocin while decreasing the *N*-GSDME/GSDME ratio (P<0.05) (Figure 3C-D). Therefore, the above results suggest that chaetocin-induced pyroptosis in gastric cancer cells was caused by the caspase 3/GSDME signaling pathway rather than the GSDMD pathway.

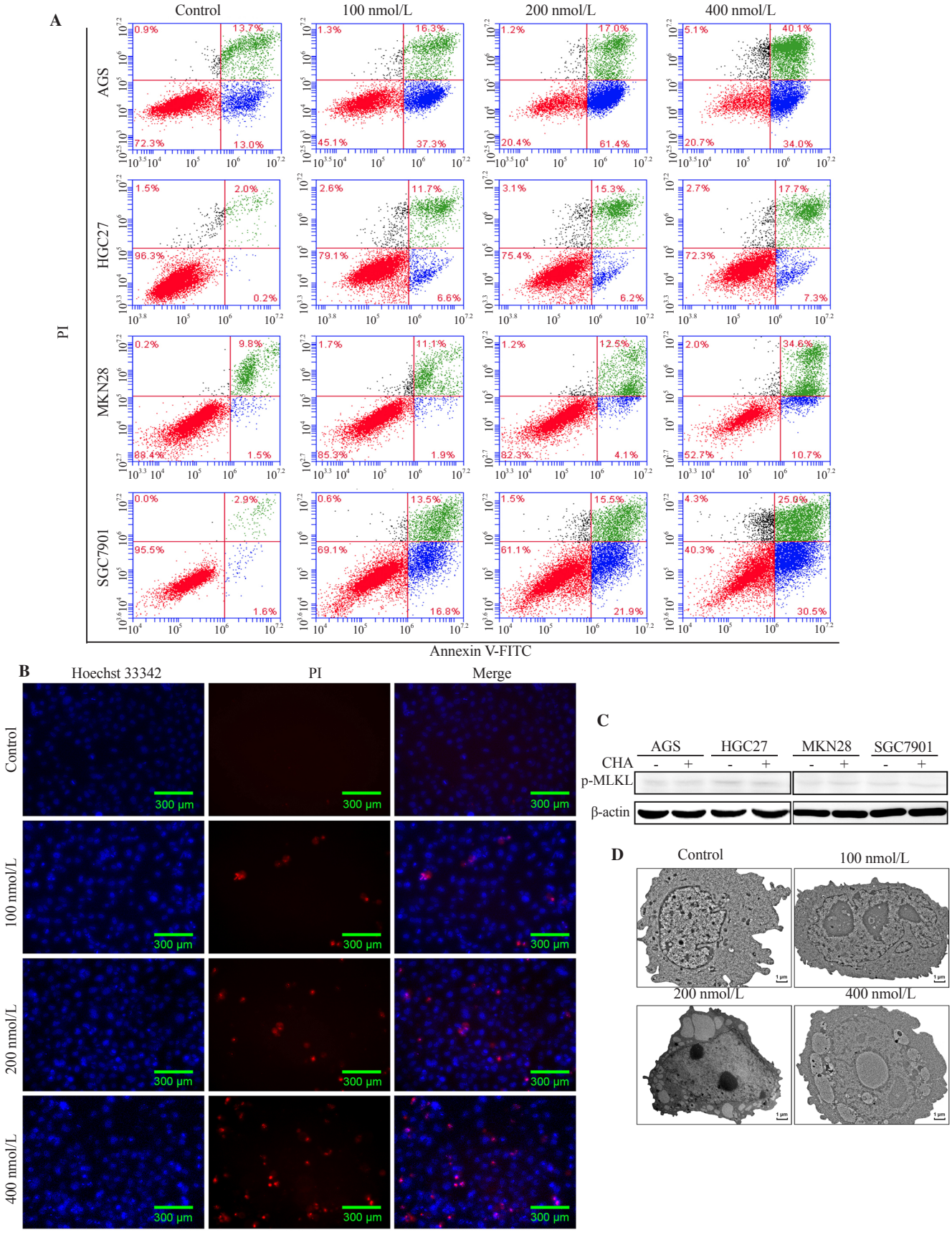

Figure 2. Chaetocin induces pyroptosis of gastric cancer cells in addition to apoptosis. (A) AGS, HGC27, MKN28, and SGC7901 were treated with 100, 200, and 400 nmol/L chaetocin for 24 h. Flow cytometry was performed with Annexin V-FITC and propidium iodide (PI) staining. (B) SGC7901 cells were stained with Hoechst 33342 and PI after 24 h treatment with chaetocin. Fluorescent images were observed under ZEISS Axio Vert.A1 inverted fluorescence microscope (magnification: 200×). (C) AGS, HGC27, MKN28, and SGC7901 were treated with 400 nmol/L chaetocin for 24 h and p-MLKL protein level was evaluated by Western blotting. (D) Ultramicrostructure of SGC7901 cells under a transmission electron microscope after treatment with 100, 200, and 400 nmol/L chaetocin for 24 h (magnification: 1 200×). CHA: chaetocin.

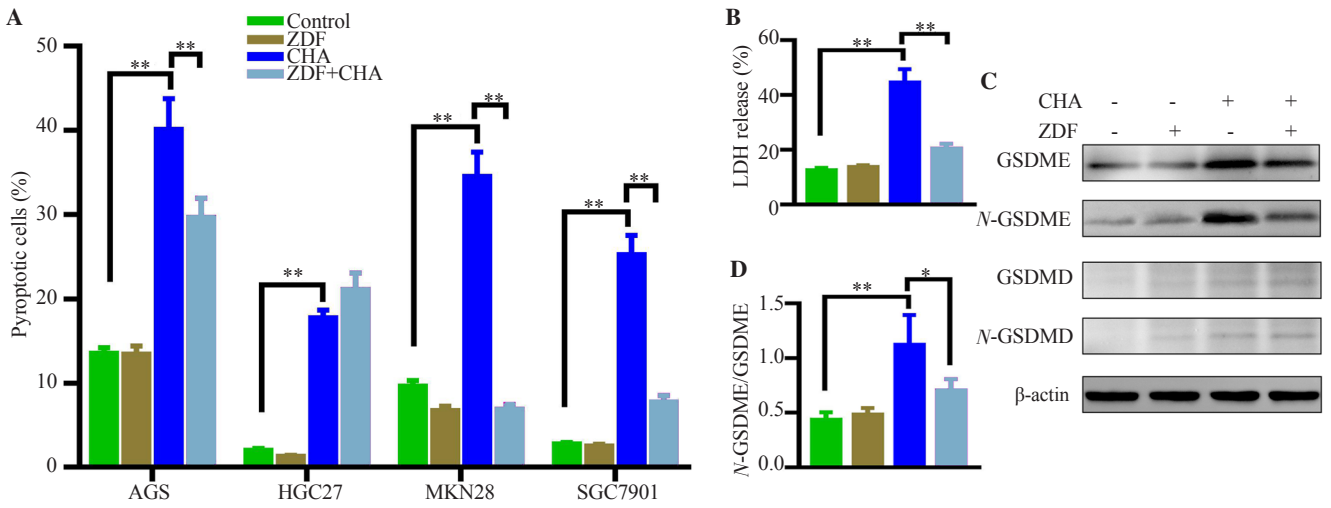

Figure 3. Caspase 3/GSDME pathway contributes to chaetocin-induced pyroptosis in SGC7901 cells. (A) AGS, HGC27, MKN28, and SGC7901 were treated with 400 nmol/L chaetocin for 24 h immediately after incubating with 50 μmol/L Z-DEVD-FMK (ZDF) for 30 min. Pyroptotic cell percentage was measured by flow cytometry with Annexin V-FITC/PI double staining. Representative results for the SGC7901 cell line are shown in (B-D) after the same treatment as in (A). (B) LDH released was detected by LDH cytotoxicity assay kit. (C) The expressions of GSDME, *N*-GSDME, GSDMD, and *N*-GSDMD were evaluated by Western blot. (D) *N*-GSDME/GSDME ratios were calculated and analyzed by ImageJ V1.51 software. Bars represent mean ± SD (n=3). $^{*}P$<0.05; $^{**}P$<0.01.

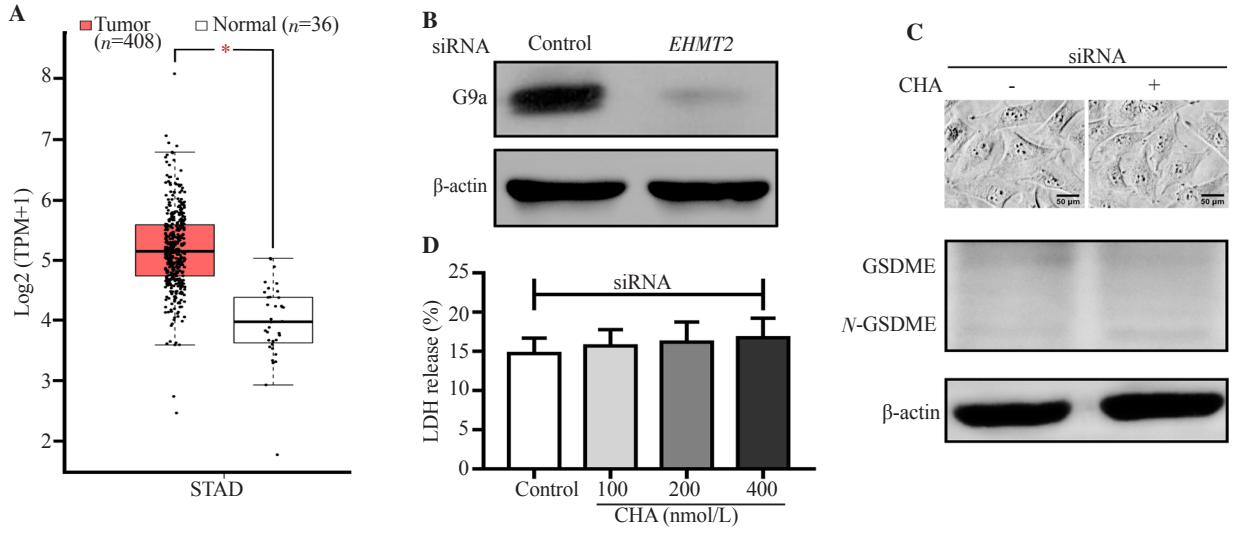

Figure 4. Silencing of the *EHMT2* gene abolishes chaetocin-induced pyroptosis. (A) Differential expression of EHMT2 in human stomach adenocarcinoma (red box) and normal gastric tissue (white box) ($^{*}P$<0.05). EHMT2 transcripts per million (TPM) were analyzed using the GEPIA website (http://gepia.cancer-pku.cn) database. (B) G9a protein was detected in SGC7901 cells by Western blot after *EHMT2*-silencing with siRNA. (C) *EHMT2*-silenced cells were treated with 400 nmol/L chaetocin for 24 h. The cellular morphology was observed (magnification: 200×). GSDME and *N*-GSDME protein levels were measured by Western blotting. (D) LDH release in *EHMT2*-silenced SGC7901 cells after treatment with 100, 200, and 400 nmol/L chaetocin. Bars represent mean ± SD (n=3).

3.4. Silencing of EHMT2 gene abolishes chaetocin-induced pyroptosis in gastric cancer cells

G9a is encoded by the gene, *EHMT2*. Differential expression of EHMT2 in gastric cancer and healthy gastric tissues was analyzed by searching the GEPIA website. EHMT2 transcript levels were found to be higher in gastric cancer tissues than in normal tissues (P<0.05; Figure 4A), indicating a potential role for G9a as a biomarker in gastric cancer. EHMT2 was knocked down by siRNA in SGC7901 cells and treatment with 400 nmol/L chaetocin for 24 h produced no abnormal morphological changes compared to the control group (Figure 4B-C). Similarly, chaetocin had no impact on GSDME and *N*-GSDME expression (Figure 4C) or LDH release in *EHMT2*-silenced SGC7901 cells (P>0.05) (Figure 4D). These data suggest that chaetocin-induced pyroptosis was inhibited in the absence of G9a in SGC7901 cells.

4. Discussion

Chaetocin can suppress growth of many tumor cell types, including myeloma, leukemia, non-small cell lung cancer, hepatocellular carcinoma, intrahepatic cholangiocarcinoma, melanoma, glioma, colon cancer, renal cancer, prostate cancer, breast cancer and ovarian cancer[16–21]. In this study, chaetocin inhibited the proliferation of four gastric cancer cell lines with different degrees of differentiation in a time-dependent manner. Chaetocin inhibition tends to be more pronounced for cells from solid tumors. Mechanisms underlying the anti-tumor activity involve the induction of apoptosis, cell cycle arrest, autophagy, and suppression of tumor cell invasion, metastasis, and angiogenesis[10,12,22–24]. The current study reported that chaetocin induced pyroptosis of gastric cancer cells in addition to apoptosis.

Cookson *et al*. initially identified pyroptosis as a novel programmed cell death mode distinct from apoptosis[25]. In addition, caspase 1/4/5/11 had been found to cleave GSDMD into *N*-GSDMD increasing membrane permeability during pyroptosis. *N*-GSDMD creates oligomerized pores in the cell membrane to release cellular contents, triggering pyroptosis and inflammatory reactions[26–28]. It was later discovered that the gasdermin family, GSDMA, GSDMB, GSDMC, and GSDME/DFNA5, were also cleaved to yield *N*-terminal proteins with similar roles to *N*-GSDMD[29–31]. As a result, the Nomenclature Committee on Cell Death redefined pyroptosis as "a type of regulated cell death that critically depends on the formation of plasma membrane pores by members of the gasdermin protein, often (but not always) as a consequence of inflammatory activation"[32]. Chaetocin raised GSDME and *N*-GSDME levels in the current work accompanied by an increase in the number of pyroptotic cells, but did not affect GSDMD and *N*-GSDMD. Caspase 3 is thought to be involved in both apoptosis and pyroptosis and to either inactivate GSDMD or activate GSDME through the cleavage of GSDME to produce *N*-GSDME which increases membrane permeability and induce pyroptosis[33,34]. Pyroptosis may be induced by the caspase 3/GSDME or the traditional GSDMD pathway in the treatment of cancers with most chemotherapeutic drugs. Caspase 3 inhibition abolished the upregulation of GSDME and *N*-GSDME caused by chaetocin, decreasing the *N*-GSDME/GSDME ratio and pyroptotic cell number. Thus, the caspase 3/GSDME pathway is responsible for chaetocin-induced pyroptosis in gastric cancer cells rather than the conventional GSDMD pathway. Further research is required to determine whether other gasdermins and associated pathways contribute to chaetocin-induced cell pyroptosis.

The reports of other researchers and our bioinformatics analysis indicate that G9a plays an important role in the formation and evolution of gastric cancer. In the present study, a lack of G9a expression could result in the abolition of pyroptosis induced by chaetocin. Thus, we infer that G9a may be one of the targets of chaetocin to induce pyroptosis of gastric cancer cells. However, the pharmacological action of chaetocin is not specific. In addition to HMTs, thioredoxin reductase 1, heat shock protein 90, and hypoxia-inducible factor-1 alpha/p300 complex have also been identified as target molecules of chaetocin[35–37]. Whether these other molecules are also involved in the chaetocin-induced regulation of pyroptosis remains to be addressed.

In conclusion, the present study shows that chaetocin suppresses proliferation of gastric cancer cells by simultaneously inducing apoptosis and pyroptosis. It activated the caspase 3/GSDME pathway by targeting G9a, resulting in increasing membrane permeability and inducing pyroptosis of gastric cancer cells. These findings give new insights into the cytotoxic mechanism of chaetocin, and lay a foundation for its further development as an anti-tumor agent and for possible combination therapy.

Conflict of interest statement

The authors declare that they have no conflict of interest.

Acknowledgments

We would like to express our gratitude to EditSprings (https://www.editsprings.cn) for the expert linguistic services provided.

Funding

This work was supported by Natural Science Foundation of Hainan Province, China (No. 820MS048).

Authors' contributions

MQH designed and performed experiments, analyzed data, prepared manuscript; GLT analyzed the data and revised the manuscript. LFH and SHT performed the experiments and analyzed the data. PZ designed experiments and revised the manuscript. All authors approved the final manuscript.

References

[1] Sung H, Ferlay J, Siegel RL, Laversanne M, Soerjomataram I, Jemal A,

et al. Global Cancer Statistics 2020: GLOBOCAN estimates of incidence and mortality worldwide for 36 cancers in 185 countries. *CA Cancer J Clin* 2021; **71**(3): 209-249.

[2] Sexton RE, Al Hallak MN, Diab M, Azmi AS. Gastric cancer: A comprehensive review of current and future treatment strategies. *Cancer Metastasis Rev* 2020; **39**(4): 1179-1203.

[3] Husmann D, Gozani O. Histone lysine methyltransferases in biology and disease. *Nat Struct Mol Biol* 2019; **26**(10): 880-889.

[4] Chae YC, Kim JY, Park JW, Kim KB, Oh H, Lee KH, et al. FOXO1 degradation *via* G9a-mediated methylation promotes cell proliferation in colon cancer. *Nucleic Acids Res* 2019; **47**(4): 1692-1705.

[5] Kerchner KM, Mou TC, Sun Y, Rusnac DV, Sprang SR, Briknarová K. The structure of the cysteine-rich region from human histone-lysine *N*-methyltransferase EHMT2 (G9a). *J Struct Biol X* 2021; **5**: 100050.

[6] Poulard C, Noureddine LM, Pruvost L, Le Romancer M. Structure, activity, and function of the protein lysine methyltransferase G9a. *Life (Basel)* 2021; **11**(10): 1082.

[7] Kumari D, Sciascia N, Usdin K. Small molecules targeting H3K9 methylation prevent silencing of reactivated FMR1 alleles in fragile X syndrome patient derived cells. *Genes (Basel)* 2020; **11**(4): 356.

[8] Rajendran L, Durgadevi D, Kavitha R, Divya S, Ganeshan K, Vetrivelkalai PM, et al. Characterization of chaetoglobosin producing *Chaetomium globosum* for the management of Fusarium-Meloidogyne wilt complex in tomato. *J Appl Microbiol* 2023; **134**(2): lxac074.

[9] Samer S, Arif MS, Giron LB, Zukurov JPL, Hunter J, Santillo BT, et al. Nicotinamide activates latent HIV-1 *ex vivo* in ART suppressed individuals, revealing higher potency than the association of two methyltransferase inhibitors, chaetocin and BIX01294. *Braz J Infect Dis* 2020; **24**(2): 150-159.

[10]Jiang H, Li Y, Xiang X, Tang Z, Liu K, Su Q, et al. Chaetocin: A review of its anticancer potentials and mechanisms. *Eur J Pharmacol* 2021; **910**: 174459.

[11]Wang H, Wen C, Chen S, Li W, Qin Q, He L, et al. ROS/JNK/C-Jun pathway is involved in chaetocin induced colorectal cancer cells apoptosis and macrophage phagocytosis enhancement. *Front Pharmacol* 2021; **12**: 729367.

[12]Ozyerli-Goknar E, Sur-Erdem I, Seker F, Cingöz A, Kayabolen A, Kahya-Yesil Z, et al. The fungal metabolite chaetocin is a sensitizer for pro-apoptotic therapies in glioblastoma. *Cell Death Dis* 2019; **10**(12): 894.

[13]Setiawati A, Candrasari DS, Setyajati FD, Prasetyo VK, Setyaningsih D, Hartini YS. Anticancer drug screening of natural products: *In vitro* cytotoxicity assays, techniques, and challenges. *Asian Pac J Trop Biomed* 2022; **12**(7): 279-289.

[14]Qian C, Jiang C, Hou J. The endometrium histopathology and cell ultrastructure in bitches with pyometra induced using progesterone and *Escherichia coli*. *Tissue Cell* 2020; **67**: 101414.

[15]Li Y, Wu A, Wang D, Yang P, Sheng B. Salidroside attenuates oxygen and glucose deprivation-induced neuronal injury by inhibiting ferroptosis. *Asian Pac J Trop Biomed* 2023; **13**(2): 70-79.

[16]Hirano T, Mori S, Kagechika H. Recent advances in chemical tools for the regulation and study of protein lysine methyltransferases. *Chem Rec* 2018; **18**(12): 1745-1759.

[17]Monte-Serrano E, Morejón-García P, Campillo-Marcos I, Campos-Díaz A, Navarro-Carrasco E, Lazo PA. The pattern of histone H3 epigenetic posttranslational modifications is regulated by the VRK1 chromatin kinase. *Epigenetics Chromatin* 2023; **16**(1): 18.

[18]Yang Z, Wang H, Zhang N, Xing T, Zhang W, Wang G, el al. Chaetocin abrogates the self-renewal of bladder cancer stem cells *via* the suppression of the KMT1A-GATA3-STAT3 circuit. *Front Cell Dev Biol* 2020; **8**: 424.

[19]Sak A, Bannik K, Groneberg M, Stuschke M. Chaetocin induced chromatin condensation: Effect on DNA repair signaling and survival. *Int J Radiat Biol* 2021; **97**(4): 494-506.

[20]Li Z, Huang L, Wei L, Hou Z, Ye W, Huang S. Chaetocin induces caspase-dependent apoptosis in ovarian cancer cells *via* the generation of reactive oxygen species. *Oncol Lett* 2019; **18**(2): 1915-1921.

[21]Kim SY, Hwang S, Choi MK, Park S, Nam KY, Kim I. Molecular mechanisms underlying the effects of the small molecule AMC-04 on apoptosis: Roles of the activating transcription factor 4-C/EBP homologous protein-death receptor 5 pathway. *Chem Biol Interact* 2020; **332**. doi: 10.1016/j.cbi.2020.109277.

[22]Liao X, Fan Y, Hou J, Chen X, Xu X, Yang Y, et al. Identification of Chaetocin as a potent non-ROS-mediated anticancer drug candidate for gastric cancer. *J Cancer* 2019; **10**(16): 3678-3690.

[23]Jung HJ, Seo I, Casciello F, Jacquelin S, Lane SW, Suh SI, et al. The anticancer effect of chaetocin is enhanced by inhibition of autophagy. *Cell Death Dis* 2016; **7**: e2098.

[24]Wojtala M, Macierzyńska-Piotrowska E, Rybaczek D, Pirola L, Balcerczyk A. Pharmacological and transcriptional inhibition of the G9a histone methyltransferase suppresses proliferation and modulates redox homeostasis in human microvascular endothelial cells. *Pharmacol Res* 2018; **128**: 252-263.

[25]Cookson BT, Brennan MA. Pro-inflammatory programmed cell death. *Trends Microbiol* 2001; **9**(3): 113-114.

[26]Coll RC, Schroder K, Pelegrín P. NLRP3 and pyroptosis blockers for treating inflammatory diseases. *Trends Pharmacol Sci* 2022; **43**(8): 653-668.

[27]Humphries F, Shmuel-Galia L, Ketelut-Carneiro N, Li S, Wang B, Nemmara VV, et al. Succination inactivates gasdermin D and blocks pyroptosis. *Science* 2020; **369**(6511): 1633-1637.

[28]Zuo Y, Chen L, Gu H, He X, Ye Z, Wang Z, et al. GSDMD-mediated pyroptosis: A critical mechanism of diabetic nephropathy. *Expert Rev Mol Med* 2021; **23**: e23.

[29]Hou J, Zhao R, Xia W, Chang CW, You Y, Hsu JM, et al. PD-L1-mediated gasdermin C expression switches apoptosis to pyroptosis in

cancer cells and facilitates tumour necrosis. *Nat Cell Biol* 2020; **22**(10): 1264-1275.

[30]Zhou Z, He H, Wang K, Shi X, Wang Y, Su Y, et al. Granzyme A from cytotoxic lymphocytes cleaves GSDMB to trigger pyroptosis in target cells. *Science* 2020; **368**(6494): eaaz7548.

[31]Deng W, Bai Y, Deng F, Pan Y, Mei S, Zheng Z, et al. Streptococcal pyrogenic exotoxin B cleaves GSDMA and triggers pyroptosis. *Nature* 2022; **602**(7897): 496-502.

[32]Galluzzi L, Vitale I, Aaronson SA, Abrams JM, Adam D, Agostinis P, et al. Molecular mechanisms of cell death: Recommendations of the Nomenclature Committee on Cell Death 2018. *Cell Death Differ* 2018; **25**(3): 486-541.

[33]Xia S, Hollingsworth LR 4th, Wu H. Mechanism and regulation of gasdermin-mediated cell death. *Cold Spring Harb Perspect Biol* 2020; **12**(3): a036400.

[34]Yao F, Jin Z, Zheng Z, Lv X, Ren L, Yang J, et al. HDAC11 promotes both NLRP3/caspase-1/GSDMD and caspase-3/GSDME pathways causing pyroptosis *via* ERG in vascular endothelial cells. *Cell Death Discov* 2022; **8**(1): 112.

[35]Wen C, Wang H, Wu X, He L, Zhou Q, Wang F, et al. ROS-mediated inactivation of the PI3K/AKT pathway is involved in the antigastric cancer effects of thioredoxin reductase-1 inhibitor chaetocin. *Cell Death Dis* 2019; **10**(11): 809.

[36]Lian B, Lin Q, Tang W, Qi X, Li J. SUV39H1 is a new client protein of Hsp90 degradated by chaetocin as a novel *C*-terminal inhibitor of Hsp90. *Biomol Ther (Seoul)* 2021; **29**(1): 73-82.

[37]Reece KM, Richardson ED, Cook KM, Campbell TJ, Pisle ST, Holly AJ, et al. Epidithiodiketopiperazines (ETPs) exhibit *in vitro* antiangiogenic and *in vivo* antitumor activity by disrupting the HIF-1alpha/p300 complex in a preclinical model of prostate cancer. *Mol Cancer* 2014; **13**: 91.

Publisher's note